Heliyon 5 (2019) e02875

Contents lists available at ScienceDirect

Heliyon

journal homepage: www.heliyon.com

Heliyon

Research article

Soil flushing pilot test in a landfill polluted with liquid organic wastes from lindane production

Aurora Santos [a,*], Carmen M. Domínguez [a], David Lorenzo [a], Raul García-Cervilla [a], Miguel A. Lominchar [a], Jesús Fernández [b], Jorge Gómez [c], Joaquín Guadaño [c]

[a] Chemical Engineering and Materials Department, Complutense University of Madrid, Spain
[b] Department of Rural Development and Sustainability, Government of Aragon, Spain
[c] EMGRISA, Empresa Para La Gestión de Residuos Industriales, S.A., S.M.P,. M.P., Madrid, Spain

ARTICLE INFO

Keywords:
Chemical engineering
Environmental chemical engineering
Soil pollution
Environmental pollution
Contaminant transport
Lindane wastes
DNAPL
Surfactant
Alluvium
Tracer
Landfill

ABSTRACT

Sites contaminated by Dense Non-Aqueous Liquid Phases (DNAPLs) containing chlorinated compounds are a ubiquitous problem caused by spills or the dumping of wastes with no concern for the environment. Their migration by gravity through the subsurface and their accumulation far below ground level make in-situ treatments the most appropriate remediation technologies. In this work, an aqueous solution containing a non-ionic and biodegradable surfactant was injected in the Sardas alluvial layer contaminated at some points with DNAPL (formed by a mixture of more than 28 chlorinated compounds) from lindane production. A volume of 5.28 m^3 of an aqueous surfactant emulsion (13 g L^{-1}) was injected at 14.5 m b g.l in the permeable layer (gravel-sand), at a flow rate of 0.6 m^3 h^{-1} and the groundwater was monitored within a test cell (3.5 m radius) built *ad hoc*. The flow of the injected fluids in the subsurface was also evaluated using a conservative tracer, bromide (130 mg L^{-1}), added to the surfactant solution. Concentration of contaminants, chloride, bromide and surfactant, surface tension and conductivity were measured at the injection point and at three monitoring points over time. High radial dispersion was noticed resulting in high dilution of the injected fluids. The surfactant was not adsorbed in the soil during the injection time, the adsorption of the surfactant took place in the meantime (15 h) between its injection and the groundwater (GW) extraction. The concentration of chlorinated compounds dissolved from the soil in the surfactant aqueous phase when equilibrium was reached (about 850 mg L^{-1}) is related to the moderate average contamination of the soil in the test cell (about 1230 mg kg^{-1}). In contrast, the extraction of the free DNAPL in the altered marls layer was highly enhanced due to the addition of the surfactant. Finally, it was found that the surfactant and the contamination did not migrate from the capture zone.

1. Introduction

Contamination of soil and groundwater by organic compounds from industrial activities has become a major problem for the environment and human health (van Liedekerke et al., 2014). Among these, the accidental release or intentional dumping of hydrophobic organic liquid phases into the environment has resulted in a separate liquid phase, termed non-aqueous phase liquids (or NAPLs), that persists in the subsurface (Siegrist et al., 2011a). When a NAPL is denser than water it is known as a dense non-aqueous phase liquid (DNAPL). Many of these DNAPLs are chlorinated compounds characterized by high toxicity, persistence in the environment, bioaccumulation and, in some cases, carcinogenesis (Council, 2013).

Due to their high density, DNAPLs can migrate through soils and groundwater until they encounter an impermeable layer that avoids further descent, producing DNAPL pools or ganglia (CLU-IN, 2016). Additionally, during their transport through the subsurface these dense phases often interact with the soil matrix, depending on the nature of the organic contaminant and the soil granulometry and composition, resulting in a significant amount of DNAPL trapped in the soil pores (Brusseau, 2013; Agaoglu et al., 2015). These hydrophobic dense organic phases can create highly residual saturation areas at depths of several tens of meters below ground level and act as sources of secondary contamination of the groundwater (Kokkinaki et al., 2013; Koch and Nowak, 2015). Sites may remain contaminated for decades after the initial discharge because of the extreme persistence of these pollutants

* Corresponding author.
E-mail address: aursan@ucm.es (A. Santos).

https://doi.org/10.1016/j.heliyon.2019.e02875
Received 7 August 2019; Received in revised form 20 October 2019; Accepted 14 November 2019

and their hydrophobic nature (Henry et al., 2003; Luciano et al., 2018).

In this context, in-situ remediation treatments with a low environmental and economic impact are required to solve these problems. However, in-situ technologies such as ISCO (In-Situ Chemical Oxidation) are limited to NAPLs dissolved in the groundwater, and are not suitable for adsorbed or residual contaminants, ganglia of NAPLs in unsaturated soils or source zone NAPLs (Dugan et al., 2010; Hoag and Collins, 2011; Siegrist et al., 2011b; Collins, 2012; Stroo et al., 2012; Brebbia, 2013; Wang et al., 2013). Moreover, when a high concentration of the pollutants is present in the aqueous phase due to saturation of the contact with the dense organic phase in-situ bioremediation is not suitable (Henry et al., 2003; McGuire et al., 2006). In-Situ Chemical Oxidation, using the simultaneous injection of oxidants and surfactants (S–ISCO), has been used for in-situ remediation technologies to remove residual NAPLs in the subsurface (Besha et al., 2018). However, if significant DNAPL masses remain in the subsurface, Surfactant-Enhanced Aquifer Remediation (SEAR) or Surfactant Enhanced Product Recovery (SEPR) can be better applied as a first step (Mulligan et al., 2001; Londergan and Yeh, 2003; Atteia et al., 2013; Acosta and Quraishi, 2014; Mao et al., 2015a; Cheng et al., 2017). With SEAR, the removal of a substantial part of the DNAPL mass in the aquifer can be achieved by injecting a surfactant solution, which sweeps across the DNAPL source zone, and the simultaneous extraction of the chemicals injected and the solubilized or emulsified DNAPL. The extracted fluids should be treated above ground in order to remove the free-product DNAPL (usually by decantation) and the pollutants dissolved in the surfactant emulsion should also be dealt with. The recovery of surfactant for reinjection is desirable when possible (Dominguez et al., 2019).

Surfactant molecules (soap) are amphoteric compounds with a polar head and a non-polar tail. Solubilization and lowering of the surface and interface tension are the main mechanisms that facilitate the transport of hydrophobic pollutants adsorbed in the solid phase to the aqueous phase. When the concentration of the surfactant is high enough, micelles with polar heads on the outside and non-polar tails on the inside are formed. Within the micelle, a hydrophobic environment that attracts organic contaminants is created and the DNAPL extracted from the soil is accumulated inside of them and the emulsion can be flushed away. The combined use of surfactants with other additives, such as organic solvents, chelating agents, salts, ligand ions or air, has been shown to be more effective at removing soil pollutants than the surfactants alone (Mao et al., 2015a). Some authors have reported that the use of foams decreases one order of magnitude the mass of surfactant required to extract a mass of DNAPL alone (Maire et al., 2015, Maire et al., 2018). Organic co-solvents are usually added to enhance the solubility of organic pollutants in the aqueous phase (Aydin et al., 2011). The review of Atteia et al. (2013) shows that the use of cosolvents can reduce to the half the amount of surfactant needed.

However, if the permeability is low, the applicability of the soil flushing technology is limited. Moreover, the adsorption of the surfactants in the soil and the possible dispersion of contaminants beyond the capture zone are concerns that should be evaluated (Paria, 2008; Kang et al., 2019). In the literature, it was found higher adsorption of non-ionic than anionic surfactants (Muherei et al., 2009). These authors found that the adsorption of Triton X100 was higher than that one of Sodium Dodecyl Sulfate. Moreover, it was noticed a high influence of soil lithology on surfactant adsorption, this adsorption being higher in shale that in sandstone. The adsorption of organic compounds on surfaces is a common finding, also studied in wastewater treatment (Şen et al., 2018; Nas et al., 2019). To safely use the technology the flushed contaminants and soil flushing fluid must be contained and recaptured (Londergan and Yeh, 2003). Thus, the transport characteristics of the injected fluid must be known. However, most of the works in literature related to soil flushing have been carried out in batches or columns, often with spiked soils, and very few studies have been carried out at pilot or field scale (Strbak, 2000; Abriola et al., 2005; Paria, 2008; Svab et al., 2009; Atteia et al., 2013; Mao et al., 2015b; EthicalChem, 2016d, EthicalChem, 2016e).

The scope of this work is to check the applicability of the SEAR technology in the remediation of a site highly polluted with DNAPL, which corresponds to liquid residue produced during the production of lindane by the company INQUINOSA (Sabiñanigo, Huesca). The residue was dumped some decades ago in two landfills near the production site: Bailin and Sardas. About thirty chlorinated organic compounds (COCs), from chlorobenzene to heptachlorocyclohexane, were identified in this DNAPL (Santos et al., 2018) with a density of about 1.5 g cm^{-3}. This dense phase has migrated through the subsurface, affecting the alluvial deposits hydraulically linked to the Gallego River (Fernández et al., 2013). The alluvium of the Sardas landfill consists in a sand gravel layer (also containing some interbedded clay) with high permeability but a low hydraulic gradient (Fernández et al., 2013) located between two low permeability layers (lime and marls). The soil is highly contaminated at some points. In addition to the DNAPL trapped in the soil pores, DNAPL pools have been found at some locations, mainly between the gravel-sand and the altered marl layer, about 16 m below ground level. This DNAPL is phase is viscous and currently difficult to extract by pumping.

The surfactant selected is non-ionic and commercial, E-Mulse 3® by EthicalChem, and was previously tested in the laboratory with the free phase. Surfactant emulsion was injected and monitored with a test cell (3.5 m radius from the injection point) built *ad hoc* in the alluvium of the Sardas landfill. The location of this test cell was selected taking into account the high level of chlorinated organic compounds measured in the groundwater in the piezometers available at the site. Values of hexachlorocyclohexanes (HCH) concentration higher than 10 mg L^{-1} suggested the presence of a DNAPL phase, free or adsorbed into the nearby soil. To study the transport of the injected fluids, a conservative tracer, bromide, was added to the surfactant solution injected.

Due to the small size of the test cell, the objective of this work was not site remediation but to acquire knowledge for the proper design of future SEAR or S–ISCO technologies at full scale in the alluvium, which should take into account the proximity of the Gallego River and the Sabiñanigo reservoir. In this sense, the dispersion of fluid injected in the alluvial layer, adsorption of the surfactant into the soil, washing capacity of the surfactant, possible mobilization of the DNAPL by the surfactant and control of the surfactant injected in the landfill have been evaluated.

2. Experimental section

2.1. Site description

This small pilot test was carried out at Sardas landfill (Sabiñánigo, Spain). The conceptual model of the site, summarized in Figure SI-1, was described elsewhere (Fernández et al., 2013). The permeable layer was a mixture of gravel and sand (and some interbedded clay). A hydraulic conductivity, K_h, of about 100 m day^{-1}, an average Darcy velocity of about 0.02 m day^{-1}, a hydraulic gradient of about 0.001, an effective soil porosity ε_L of 0.1–0.12 and a soil density of about 2.5 kg L^{-1}were previously determined in this layer.

The Sabiñanigo Reservoir is located nearby (about 150 m from the cell site). The opening or closing of the dam produces changes in the water level of the reservoir and affects the piezometric level of the wells in the landfill.

A surfactant aqueous solution was injected in a well, called PS14B, which was built *ad hoc* for this experiment. The selection of the well location was based on the concentration of HexaChlorocycloHexanes (HCHs) in the numerous monitoring wells already available in the alluvium (shown in Figure SI-2 of the supplementary information). The contamination of the groundwater measured at the same depth in the gravel-sand layer at wells located short distances away (less than 10 m) varies by two or three orders of magnitude. This indicates that free DNAPL or highly contaminated soil must be near the wells and contain high concentrations of HCHs in the groundwater.

Two new monitoring wells, PS14C and PS14D, were built at 2.5 and 3

m from the injection point. The test cell also uses an old monitoring well, PS14, which was drilled 15 years ago. It is located 3.5 m from the PS14B well and a HCH concentration of about 10 mg L^{-1} was measured in the groundwater samples taken at this well. This test cell, with a 3.5 m radius from the injection point (well PS14B), was located in the alluvium as shown in Figure SI-2 of the Supplementary Information. The site stratigraphy, shown in Figure SI-3, was obtained from the borehole drilled for PS14B. Four layers can be differentiated: an anthropic fill (0–4.8 m b g.l.), a homogeneous silt layer (4.40–12.50 m b g.l.), a gravel-sand layer of about 3 m with some clay matrix interbedded (12.50–15.50 m b g.l.) and an altered marl layer below this layer (>16 m b g.l). A scheme for the test cell is shown in Fig. 1. The gravel-sand layer was permeable, while the lime and marl layers have low permeability.

The stratigraphy from borehole drillings PS14, PS14C and PS14D was similar to that described for PS14B. As can be seen in Fig. 1, wells PS14B, C and D were screened 1 m in the silt layer, in the entire depth of the gravel-sand layer (3 m) and 1 m in the altered marls. In all cases, the boreholes were only screened in the saturated zone. Because PS14 was an existing borehole, built some years before, screening covered the entire depth of the silt and gravel-sand layers, and 1 m in altered marl (total length screened 10 m). During the borehole drilling for PS14D a DNAPL phase was found in the interface between the gravel-sand and the altered marl layers as indicated in Fig. 1.

As previously mentioned, in addition to the wells built *ad hoc* in the test cell, many other piezometers were already available in the landfill to monitor the GW contamination, as can be seen in Figure SI-2.

2.2. Surfactant injection and groundwater extraction

The surfactant used was a commercial cosolvent-surfactant mixture called E-Mulse 3 ® from EthicalChem. E-Mulse 3 ® was selected because it is a biodegradable and non-toxic surfactant. This surfactant was chosen elsewhere among other non-ionic and biodegradable options, such as Tween-Span, in the remediation of a soil contaminated with aged fuel (Lominchar et al., 2018). Moreover, this surfactant has been widely tested in SEAR studies at field scale as can be seen in https://www.ethicalchem.com/remediation-case-studies (EthicalChem, 2019) and in the review of Besha et al. (2018). It is soluble in water and highly stable under normal conditions, with a yellowish color, citrus odor and slight viscosity. It is composed of non-ionic surfactants (60–90%) and citrus terpenes (10–40%), specifically, limonene (CAS: 94266-47-4). The critical micellar concentration of the surfactant was determined in this work, with a value of 80 mg L^{-1}.

A container with a capacity of 10 m^3 was filled with 5.76 m^3 of tap water, 13 g L^{-1} of surfactant and 130 mg L^{-1} of bromide. Sodium bromide was purchased from Fluka. The cistern is shown in Figure SI-4. Conductivity of the solution in the container was 520 mS cm^{-1}, chloride concentration 125 mg L^{-1} and interfacial tension 33 mN m^{-1}. This solution was injected (at zero time) in well PS14B at a depth of 14.5 m b g.l (in the gravel-sand layer, therefore, in the saturated zone) using a flexible 1-inch PVC hose (Tiger Flex) and an electric transfer pump. The flow rate was measured over time and was approximately 0.6 m^3 h^{-1}. The aqueous surfactant solution was pumped for 8.83 h, until 5.28 m^3 from the container was injected.

Monitoring wells PS14, PS14C and PS14D were periodically sampled at a depth of about 14.5 m with a Mini-Typhoon® DTW 40ft12V electric pump. About 4 L of liquid was previously purged before taking a sample to ensure complete renovation of the liquid in the sampling tube. After purging, a volume of about 200 mL was sampled and COC concentration, surfactant concentration, bromide and chloride concentration, conductivity and interfacial tension were measured. Samples were taken at each well and at several heights in the alluvial layer before the injection took place and 40 min after the injection concluded.

15 h after injecting the 5.28 m^3 of aqueous solution containing the surfactant and the tracer, groundwater extraction began. GW extraction was carried out at a flow rate of about 1 m^3 h^{-1} from well PS14B (at a depth of 14.5 m) for 9.58 h, using the same tube and pump described above. GW samples from the discharge tube placed at PS14B and from the monitoring wells PS14, PS14C and PS14D were taken at several times. The same parameters described in the injection were determined in the GW samples. The GW extracted was fed first into a lamellar decanter and then the effluent was sent to the container as shown in Figure SI-4. Initial GW samples were also taken at 14.5 m before the GW extraction was performed.

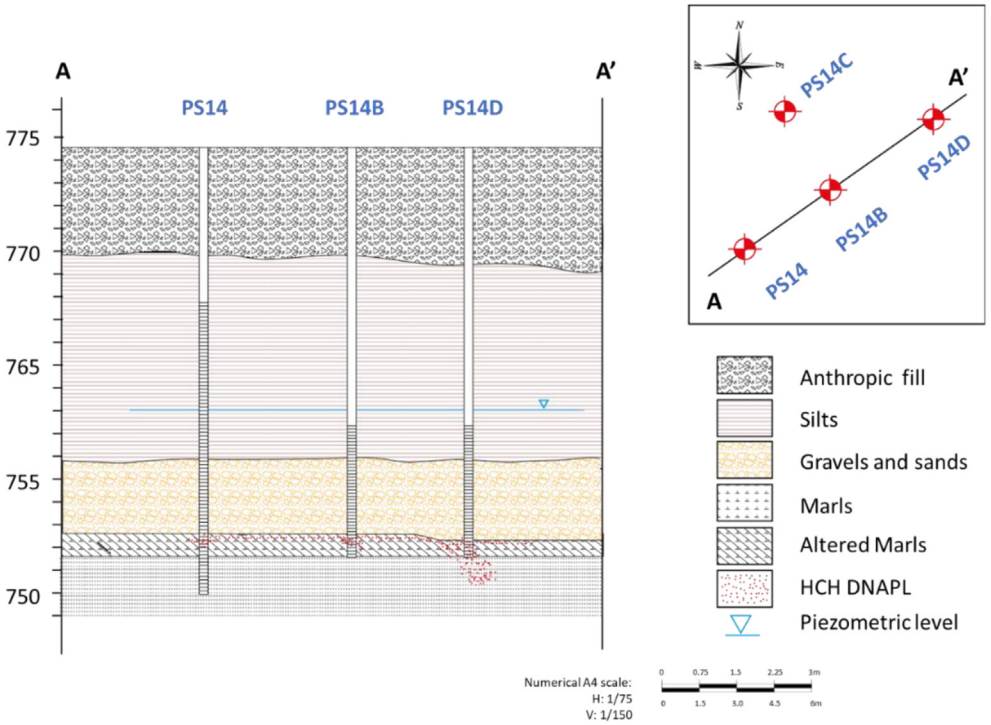

Fig. 1. Scheme of the test cell built ad hoc in the alluvium of the Sardas landfill for tracer experiments.

2.3. Flushing with water

In order to assure that neither the surfactant nor higher levels of solubilized COCs than those initially present in the site remained in the GW due to the surfactant injection, additional injections of tap water with simultaneous GW extraction were carried out.

The first injection of clean tap water took place 13.5 h after concluding the first GW extraction. Tap water was injected for 5 h in wells PS14, PS14C and PS14D and simultaneously extracted in PS14B to recover the remaining fluid injected in the test cell during surfactant injection. Extraction from PS14B started 1 h before the tap water was injected in wells PS14, PS14C and PS14D. The flow rate used was different in each well.

A second instance of simultaneous injection of tap water in PS14, PD14C and PS14D and extraction from PS14B was carried out 17.5 h after the first one was completed.

During the injection of tap water in PS14, PS14C and PS14D with simultaneous GW extraction from PS14B, samples were also periodically taken in the four wells at 14.5 m b g.l and the parameters listed above were analyzed.

Table SI-1 summarizes the schedule and flowrates of all injections and extractions.

Further monitoring of COC and HCH concentrations in the GW of the test cell wells was conducted 15 days and one month after the surfactant injection took place. Moreover, other monitoring wells in Figure SI-2 located in the vicinity of the test cell were sampled at one, two and four months after the pilot test was finished and the values of contaminant concentration, mainly HCH concentration as a control parameter, were compared with those measured previously from surfactant injection.

2.4. Analytical methods

2.4.1. Extraction of COCs from soil samples

The soil from the new boreholes drilled was collected and stored at room conditions in closed core boxes for three days, when the samples were analyzed. Moisture content was about 15%. To do this, soil collected at several depths in the alluvial layer was sieved to obtain the fine fraction <2 mm. About 5 g of soil was dried by mixing it with anhydrous sodium sulfate and milled in a ceramic mortar. 25 ml of a mixture of hexane:acetone 1:1 was then added and the resulting mixture was poured in a microwave extraction device (Milestone Ethos One). COC extraction from soil was accomplished following EPA method 3546. The temperature program started with a temperature ramp from room temperature to 110 °C in 15 min, and this temperature was maintained for 15 min, under a maximum power of 1000 W. At the end of the extraction procedure, approximately 15 ml of the organic phase was recovered from the supernatant, filtered with a 0.45 μm filter and analyzed by GC/MS and GC/FID/ECD. At each time (during injection and extraction events), three groundwater samples were taken from wells PS14, PS14B, PS14C and PS14D, and the concentration of COCs, surfactant, bromide and chloride, as well as the conductivity, were measured for the three samples. Differences in the analytical results were always lower than 5% and the average values have been used in the following sections.

2.4.2. Extraction of COCs from GW samples

COCs in groundwater samples with very low surfactant concentration (surface tension higher than 45 mN m^{-1}) were extracted with hexane. To do this, a volume of 8 mL of aqueous phase was added to 2 mL of hexane in a 10 mL GC vial and sonicated for 10 min. Then, the supernatant organic phase was taken and analyzed by GC/MS and GC/FID/ECD. In the cases in which the surface tension of the groundwater sample was lower than 45 mN m^{-1}, the groundwater sample was diluted 1:10 (in volume) with MeOH and directly analyzed by GC/FID/ECD.

2.4.3. COC analysis

The analytical methods for COCs quantification were developed elsewhere (Santos et al., 2018). The same methods for GC/MSD and GC/FID/ECD analysis than those reported in the previous work have been used here with the only difference that in the present case the injection volume was 2 μL instead 1 μL.

2.4.4. Inorganic species in GW

The concentration of the conservative tracer (bromide anion) and chloride (anion naturally present in the groundwater of the site) in the GW samples taken during the analyses were determined using an ionic chromatograph (Metrohm 761 Compact IC) with anionic chemical suppression, together with a conductivity detector. A Metrosep A SUPP5 5–250 column (25 cm length, 4 mm diameter) as a stationary phase was used and 250 μL of the sample was injected. The mobile phase was an aqueous solution of 3.2 mM of Na_2CO_3 and 1 mM of $NaHCO_3$ at a flow rate of 0.7 ml min^{-1}. A filtering device (0.45 μm) was included in the sample injection system. If necessary, the GW samples were diluted with Milli-Q water prior to their analysis. Standard solutions of sodium chloride (NaCl, Sigma-Aldrich) and sodium bromide (NaBr, Honeywell Fluka) were used for calibration.

The conductivity of the samples was also measured in the field with a portable pH/conductivity unit (Model 914 pH/Conductometer, Metrohm). Additionally, to get an estimation of the evolution of the test in real time, bromide concentrations were also measured in the field using an ion selective electrode (ISE) of bromides (crystal membrane electrode, Metrohm). Prior to the analysis, groundwater samples were diluted (1:2 in volume) using a TISAB (total ionic strength adjustment buffer) solution of KNO_3 (1 M).

2.4.5. Surfactant concentration and surface tension (ST)

The surface tension (ST) of the samples was measured using a Krüss tensiometer. However, ST cannot be used to determine the surfactant concentration while it remains almost constant (about 33 mN m^{-1}) when the surfactant concentration is above its critical micelle concentration (CMC). The surfactant concentration in the GW sample was calculated with a parameter called equivalent surfactant concentration (ESC) defined and determined using a method developed elsewhere (Dominguez et al., 2019). To calculate the ESC value, progressive dilutions were conducted of the samples containing surfactant until a value of ST slightly higher than that corresponding to the CMC of the surfactant is reached (the CMC of E-Mulse 3 ® was determined as 85 mg L^{-1} and the corresponding ST was 34 mN m^{-1}). The concentration of limonene, the co-solvent present in the commercial mixture E-Mulse 3 ®, was determined by GC/FID. To do this, a calibration of limonene was made preparing solutions of this compound (purchased to Sigma-Aldrich, analytical grade) in methanol. Limonene was eluted between 1,4 DCB and 1,2 DCB, as can be seen in the GC/FID chromatogram shown elsewhere (Santos et al., 2018). A mass percentage of limonene in the commercial surfactant-cosolvent mixture E-Mulse 3 ® about 15% was determined using this calibrate.

3. Results and discussion

3.1. Contamination of the soil in the test cell in the alluvial layer

The contamination of the soil obtained in the new boreholes drilled in the test cell was analyzed at different depths of the gravel-sand layer. Results are shown in Table 1 for wells PS14B and PS14D. In this table, the contamination of the soil in the contact area between the alluvial layer and the altered marls is also shown. No other significant concentrations of contaminants than those in this table were found by GC/MS or GC/FID/ECD. As can be seen, highly contaminated soil was found in the alluvial layer of the test cell. The COC content found in the soil at different depths varied greatly, but there was no correlation between depth and COC content. In wells PS14B and PS14C, the soil in contact between the

Table 1
Soil Characterization in the alluvial layer of the test cell (Wells PS14B and PS14D) (b.d.l. = below detection limit with the calibrate used).

WELL	**PS14B**							**PS14D**						
depth (m) b.g.l	12.5–13.0	13.0–13.5	13.5–14.0	14.0–14.5	14.5–15.0	15.0–15.5	15.5–16.0	12.5–13.0	13.0–13.5	13.5–14.0	14.0–14.5	14.5–15.0	15.0–15.5	15.0–16.0
C mg kg^{-1} soil	**Alluv.**	**Alluv.**	**Alluv.**	**Alluv.**	**Alluv.**	**Alluv.**	**Contact Alluv-Marls**	**Aluv.**	**Aluv.**	**Aluv.**	**Aluv.**	**Aluv.**	**Aluv.**	**Contact Alluv-Marls**
CB	5	21	73	19	2	51	5	15	5	b.d.l.	b.d.l.	b.d.l.	b.d.l.	38
1,3 DCB	b.d.l.	1	5	1	b.d.l.	b.d.l.	b.d.l.	1	b.d.l.	b.d.l.	b.d.l.	b.d.l.	1	9
1,4 DCB	7	35	126	28	4	25	13	31	24	1	4	3	26	311
1, 2 DCB	7	37	131	26	4	22	12	32	20	2	4	3	33	298
*1,3,*5 TCB	b.d.l.	2	6	1	0	b.d.l.	b.d.l.	1	2	b.d.l.	1	b.d.l.	4	21
*1,2,*4 TCB	26	152	490	104	21	79	29	91	114	28	135	45	338	1767
*1,2,*3 TCB	4	27	81	17	4	18	7	18	21	6	32	11	64	345
TetraCBsa	18	82	233	53	17	102	11	27	68	26	198	57	229	904
TetraCBs_B	30	126	345	76	29	190	17	40	103	40	344	95	341	1316
PentaCXa	8	54	113	23	21	106	3	11	17	10	108	27	79	346
PCB	4	11	29	7	4	24	1	2	9	4	41	11	30	104
PentaCXb	8	31	101	16	13	79	1	7	25	13	139	39	89	403
PentaCXc	2	11	22	5	3	22	b.d.l.	1	b.d.l.	b.d.l.	b.d.l.	b.d.l.	b.d.l.	b.d.l.
HexaCXa	2	7	28	2	3	23	b.d.l.	2	4	3	31	9	21	87
PentaCXd	2	b.d.l.	22	b.d.l.	2	b.d.l.	b.d.l.	2	3	2	20	4	9	45
PentaCXe	b.d.l.	1	1	b.d.l.	b.d.l.	1	b.d.l.	b.d.l.	1	b.d.l.	b.d.l.	b.d.l.	b.d.l.	b.d.l.
HexaCXb	b.d.l.	b.d.l.	7	b.d.l.	b.d.l.	b.d.l.	b.d.l.	b.d.l.	b.d.l.	b.d.l.	b.d.l.	b.d.l.	b.d.l.	b.d.l.
HexaCXc	b.d.l.	1	b.d.l.	b.d.l.	b.d.l.	b.d.l.	b.d.l.	b.d.l.	b.d.l.	b.d.l.	b.d.l.	1	b.d.l.	b.d.l.
alpha HCH	19	123	284	50	38	268	6	13	76	37	444	124	241	131
HexaCXd	b.d.l.	b.d.l.	b.d.l.	b.d.l.	b.d.l.	b.d.l.	b.d.l.	b.d.l.	b.d.l.	b.d.l.	b.d.l.	b.d.l.	b.d.l.	b.d.l.
beta HCH	b.d.l.	b.d.l.	b.d.l.	b.d.l.	b.d.l.	b.d.l.	b.d.l.	b.d.l.	b.d.l.	b.d.l.	1	b.d.l.	b.d.l.	1
gamma HCH	66	482	942	158	272	916	15	41	270	134	1600	443	808	2477
HeptaCH1	22	167	617	77	78	486	2	13	145	81	1077	263	609	1738
delta HCH	26	107	296	54	41	186	2	10	100	53	725	187	382	1083
epsilon HCH	6	26	78	12	8	58	2	4	23	11	132	38	34	240
HeptaCH2	7	53	213	25	25	173	1	5	51	27	405	100	228	757
HeptaCH3	3	29	89	14	4	88	1	2	29	17	230	62	126	404
Total HCHs	**116**	**737**	**1601**	**274**	**359**	**1428**	**26**	**69**	**470**	**235**	**2902**	**792**	**1465**	**3932**
Total COCS	**273**	**1582**	**4332**	**769**	**592**	**2917**	**132**	**369**	**1109**	**496**	**5670**	**1522**	**3691**	**12825**

alluvial and marl layers had a lower COC content than that found in well PS14D. This is in agreement with the appearance of a free dense organic phase in PS14D in the alluvial-marl contact when the borehole was drilled, as explained in the experimental phase. The composition and aspect of this free DNAPL is shown in Table SI-3 and was similar to other DNAPLs from the site previously analyzed (Santos et al., 2018). In Table SI-3, the acronym of each COC is also provided. The COC content in this table explains more than 95% of the DNAPL mass. As can be seen, the same COCs found in the free DNAPL appear in the soil. However, as the soil samples were partially dried during storage and sieving, the more volatile compounds, such as Chlorobenzene (CB), Dichlorobenzenes (DCBs) and Trichlorobenzenes (TCBs), were partially lost. Losses for these compounds were about 90, 50 and 15%, respectively. However, most of the HCHs, HeptaChlorocyclohexanes (HeptaCHs) and Pentaclorocyclohexenes (PentaCXs) remained in the soil due to their lower vapor pressure.

3.2. *Profile species in the test cell of the alluvial layer during surfactant and tracer injection*

Initial values of bromide (Br^-), chloride (Cl^-), conductivity (k) and surface tension (ST) were measured at three depths in the alluvial layer in wells PS14, PS14B, PS14C and PS14D. Results are summarized in Table SI-4. As can be seen, high chloride and conductivity values are found while the bromide in the GW of the site is around zero and the ST is around 72 mN m^{-1}.

In Fig. 2, the profiles of dimensionless bromide (Fig. 2a), dimensionless surfactant (Fig. 2b), the ratio of dimensionless surfactant to bromide (Fig. 2c), COCs in groundwater (Fig. 2d) and HCHs in groundwater (Fig. 2d) during the injection are shown. The GW samples were obtained at a depth of about 14.5 m b g.l in wells PS14C (2.5 m from PS14B), PS14D (3 m from PS14D) and PS14 (3.5 m from PS14B).

The dimensionless bromide and surfactant concentrations are calculated as the ratio between the concentrations of these compounds in the GW sample ($C_{surfact}$, C_{Br}^-) and their concentrations in the tank containing the solution injected ($C_{surfact\ tank}$, $C_{Br\ tank}$). The dimensionless surfactant/bromide, $R_{S/Br}$ ratio is defined by Eq. (1):

$$R_{S/Br} = \frac{\frac{C_{surfact}}{C_{surfact\ tank}}}{\frac{C_{Br^-}}{C_{Br\ tank}}} \quad (1)$$

As can be seen in Fig. 2, an increase in bromide and surfactant concentrations was found first in well PS14C, then in PS14D and finally in PS14, in accordance with the distance of these wells to the injection point (PS14B). However, high radial dispersion was found, explaining the profiles obtained during the injection and shown in Fig. 2, that do not fit those expected in an advective flow (or plug flow). If the flow of the injected fluid only had an advective component, a step in the bromide and surfactant concentration from zero to the value of the corresponding concentration in the tank could be predicted at the times calculated by the following expression:

$$t_{PF} = \left(\frac{V_{void_{Rwell}}}{Q_{inj}}\right) = \left(\frac{\pi L \varepsilon_L R_{well}^{\ 2}}{Q_{inj}}\right) \quad (2)$$

where $V_{void_{Rwell}}$ is the volume of voids (pores) in the cylinder of the alluvial layer comprised from the injection point well considered, Q_{inj} is the injected flow rate (Q_{inj}=0.6 m^3 h^{-1}), ε_L, the average effective porosity, (about 0.12), L the axial length of the permeable layer (L = 3 m) and R_{well} the distance of the corresponding well to the injection point (PS14B). Values of t_{FP} are also shown in the caption of Fig. 2. As can be seen, in wells PS14C, PS14D and PS14 bromide and surfactant concentrations began to rise at much lower levels than those predicted by the advective flow model (t_{FP}) confirming, in this case, the importance of radial dispersion. The significant radial dispersion of the fluid injected can be explained by the high permeability of the alluvial layer (a hydraulic

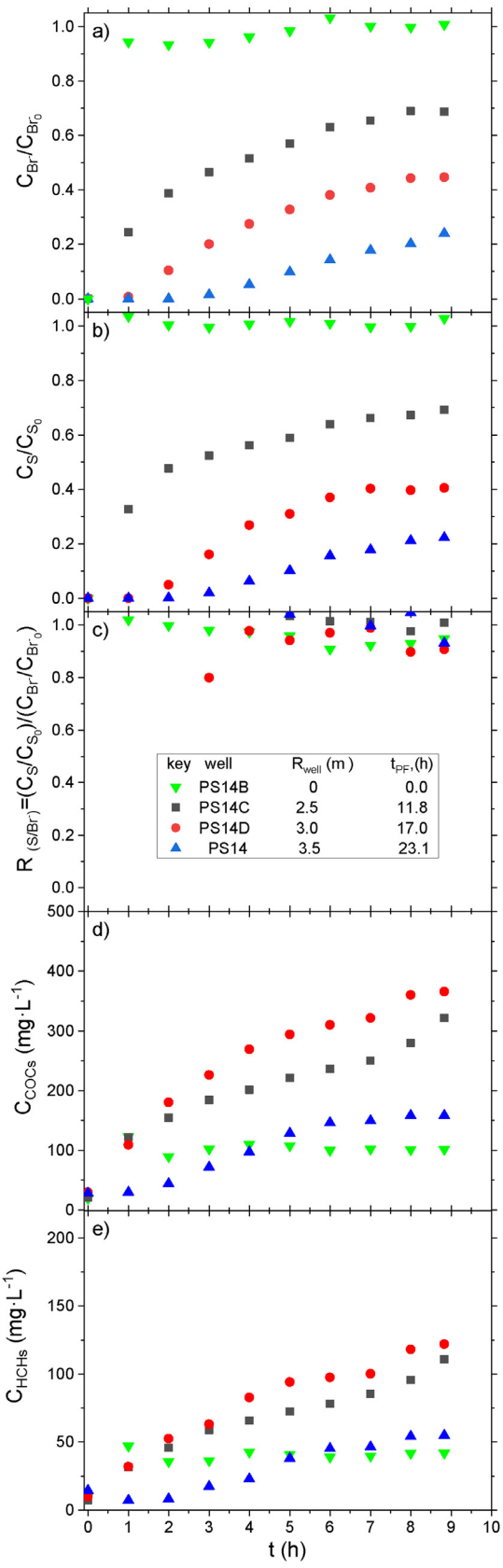

Fig. 2. Profiles of a) dimensionless bromide, b) dimensionless surfactant c) Ratio of dimensionless surfactant to bromide d) COCs in groundwater and e) HCHs in groundwater in wells PS14C (2.5 m from PS14B), PS14D (3 m from PS14D) and PS14 (3.5 from PS14B).

conductivity *Kh* of about 100 m day^{-1} was previously determined).

In Fig. 2c, it can be seen that the ratio of the dimensionless profiles of bromide and surfactant $R_{S/Br}$, defined in Eq. (1), is only slightly lower than unity during the injection. Bromide has shown to be a conservative tracer, which means that the surfactant has not been significantly adsorbed in the soil during the injection. Due to chloride concentration and conductivity values in the fluid injected are lower than in GW, decreasing profiles for conductivity and chloride concentration (data not shown) in the GW samples taken at each well during the injection were obtained.

As can be seen in Fig. 2d, the concentration of COCs in groundwater during the injection increases at each well over time except in well PS14B. The constant value obtained at PS14B is explained because at the injection point the residence time of the injected fluid is quite low and it has no COCs. The concentration of COCs in the GW at 14.5 m b g.l in well PS14D is the highest of the four wells. In Fig. 3, the values of the COCs (a) and HCHs (b) in the GW for wells PS14C (2.5 m from PS14B), PS14D (3 m from PS14B and PS14 (3.5 from PS14B) are plotted against the corresponding surfactant concentration measured in the wells. As can be seen, in spite of the fact that a lower surfactant concentration is measured in PS14D than in PS14C, the highest COC and HCH concentrations in the emulsion are detected in PS14D. This can be explained by the presence of free DNAPL in the altered marls that was found in PS14D during the borehole drilling. In addition, there is a longer distance between PS14B and PS14D than between PS14B and PS14D, which means a higher contact time between the polluted soil and the surfactant aqueous solution. As the contact time between soil and the aqueous phase containing the surfactant increases, the COCs dissolved in the aqueous phase also increase. A similar reason could be proposed to explain the higher COC and HCH concentrations vs. surfactant in PS14 in relation to those found in PS14C.

40 min after the injection of the surfactant was completed (the injection lasted for 8.33 h), GW samples were taken in the four wells at three different depths in the alluvial layer (depths for each well are summarized in Table SI-4). Values measured for bromide (mg L^{-1}), surfactant (g L^{-1}), ratio of the surfactant to bromide dimensionless concentration defined in Eq. (1), COCs (mg L^{-1}) and HCHs (mg L^{-1}) are shown in Fig. 4 a, b, c, d, e respectively.

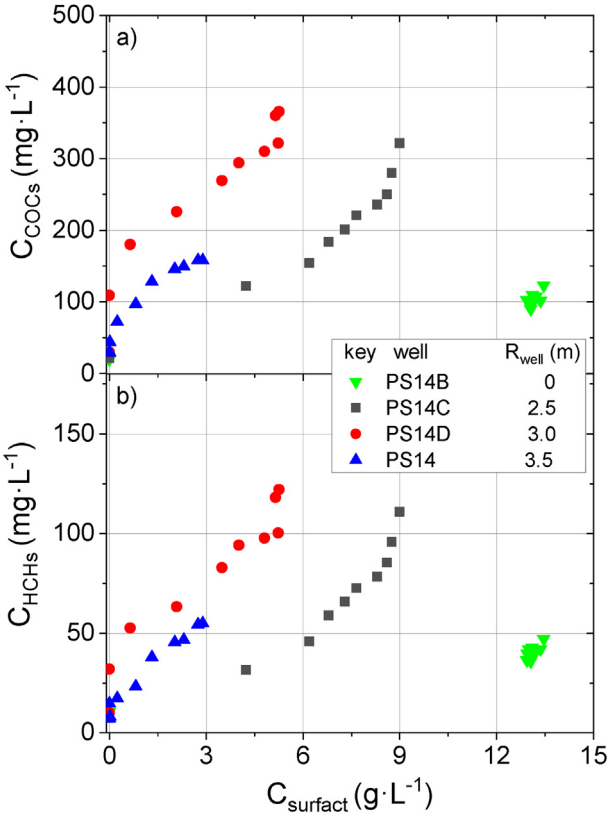

Fig. 3. Profiles of COCs a) and HCHs b) vs. surfactant concentration in groundwater in wells PS14C (2.5 m from PS14B), PS14D (3 m from PS14D) and PS14 (3.5 from PS14B) during injection.

However, values for the GW at the bottom of PS14D (16 m b g.l, corresponding to the contact between the gravels and the altered marls) could not be obtained because the presence of DNAPL at this point during sampling, as shown in Fig. 5. This DNAPL was not noticed at this depth during GW sampling before the surfactant was injected. The DNAPL in the sampling tube showed a low viscosity and was easily emulsified. The surfactant content in this DNAPL extracted at PS14D was measured obtaining a value of 4.3 g of DNAPL surfactant/kg. This can be considered the cause of the decrease in DNAPL viscosity, facilitating its extraction and increasing its emulsification capacity in the aqueous phase.

As can be seen in Fig. 4, once the injection of the surfactant stops, the concentration of COCs and HCHs does not increase in wells PS14, PS14C and PS14D. It can be assumed that the equilibrium of the aqueous emulsion with the soil in the alluvial layer was reached at the corresponding soil and surfactant conditions in these wells. The significant increase in the concentration of COCs in the aqueous phase at well PS14B 40 min after completing the injection (about 840 mg L^{-1}) can be explained by the higher surfactant concentration in this well (average 7.6 g L^{-1}).

Taking the concentration of COCs dissolved 40 min after completing the injection (840 mg/L), with a soil porosity of 0.12 and soil density of 2.5 kg L^{-1}, the mass of COCs in the surfactant aqueous solution in the pore volume per kg of soil can be calculated. Using the average COC content with the depth in the soil in the gravel-sand layer in PS14B shown in Table 1 (1230 mg kg soil^{-1}) it can be seen that about 3.5 % of the initial COCs in the mass of soil was in the aqueous surfactant solution in the pore volume of this soil.

The solubilization achieved by the surfactant is also moderate. S–ISCO treatment could be also evaluated as a better alternative for the remediation of the soil in the alluvial layer. Other studies found in the literature have reported that more than 80% of the NAPL phase, adsorbed or trapped in pores, has been removed injecting between 3-10 pore volumes of the surfactant solution (20–60 g L^{-1}) (Sahoo et al., 1998; Abriola et al., 2005; Lee et al., 2005; Paria, 2008; Mao et al., 2015a). In those studies, flushing with surfactant solutions was applied to soils more contaminated that the soil of the alluvial layer of the present work.

As can be seen in Fig. 4, when the injection stops there is a decrease in the concentration of bromide, surfactant, HCHs and COCs at the sample point located at the bottom of the alluvium in wells PS14, PS14B and PS14C. This is more evident in PS14B where a higher stratification depth is noticed. In agreement with the bromide and surfactant decrease, the rise in the chloride and conductivity was measured.

While the natural hydraulic gradient of the alluvial layer is quite low (0.001), this decrease could be explained by higher dispersion taking place at the bottom of the layer when the injection ended. Moreover, the presence of the Sabiñanigo dam has a strong influence on the piezometric water level, as can be deduced from Figure SI-1. Previously, and during the injection, the reservoir's water table was continuously increasing as shown in Figure SI-5, inducing an increase in the piezometric water level (only data for PS14B is shown but similar values were obtained in wells PS14, PS14C and PS14D). Furthermore, as can be seen in Figure SI-5, the piezometric level at PS14B continued rising after the injection ended, which clearly proves the influence of the reservoir's water table on the piezometric water levels in the landfill. Water levels in piezometers PS14, PS14C and PS14D during injection and extraction were similar to each other and also similar to that measured in PS14B (data for PS14C and PS14B is shown in Figure SI-5 as an example).

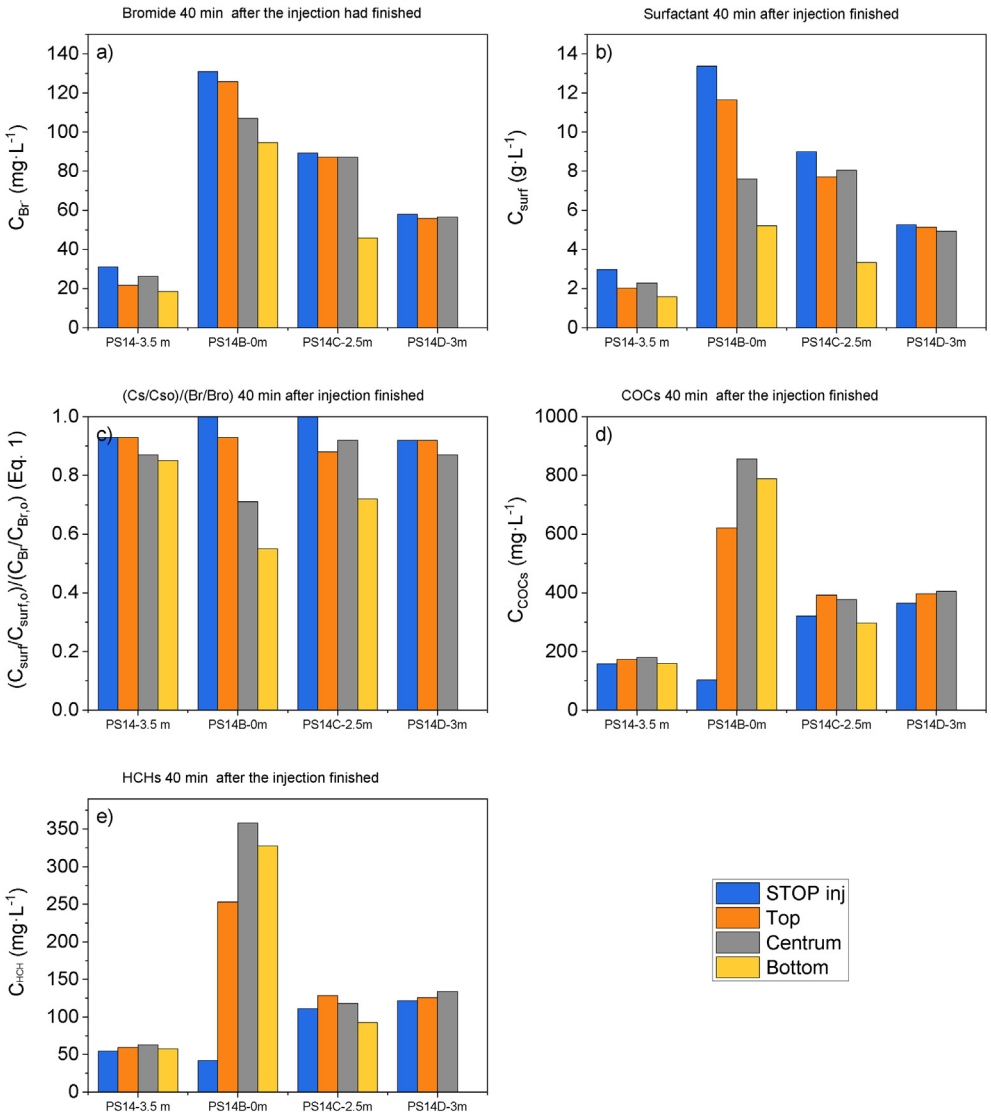

Fig. 4. Profiles of a) Bromide (mg L^{-1}) b) Surfactant (g L^{-1}) c) Ratio in Eq. (1) d) COCs (mg L^{-1}) and e) HCHs (mg L^{-1}) at three depths (Table SI-4) in each well 40 min after the injection of surfactant finished.

3.3. Profiles of the species in the test cell of the alluvial layer during extraction

As described in the Experimental Section, GW extraction began 15 h after the injection of the surfactant had ended and lasted 9.0 h at a flow rate of about 1 m^3 h^{-1}, as summarized in Table SI-1. Values of conductivity, surface tension, chloride, bromide, surfactant, COC and HCH concentrations in the GW samples taken at different times at each well (depth 14.5 m b g.l) are summarized in Table SI-2.

For comparison purposes, the corresponding values obtained at 14.5 m b g.l. and 40 min after the surfactant injection concluded (14.3 h before the extraction began) are also summarized in Table SI-2. As can be seen, between the end of the injection of the surfactant aqueous solution and the beginning of the GW extraction, a significant decrease in surfactant concentration in the wells took place. However, the change in the bromide concentration in the meantime between the end of injection event and the beginning of the GW extraction was remarkably lower than the relative decrease notice for the surfactant concentration in that period. It can therefore be inferred that the surfactant was adsorbed into the soil over this time.

Bromide and surfactant concentrations at each well decrease as the extraction time increases. Accordingly, COC and HCH concentrations in the aqueous phase decrease and conductivity and chloride concentrations in the aqueous phase increase because the GW is entering the test cell during extraction from PS14B. As can be seen, the surface tension does not increase in line with the surfactant decrease, while the CMC of the surfactant is 80 mg L^{-1}. Furthermore, as shown in Fig. 6, a similar relationship is noticed in the four wells between surfactant concentration in the aqueous phase and COC or HCH concentrations solubilized from the soil in the alluvium. Only data in PS14B obtained at the shorter times seems to go against the trend.

A mass balance of the tracer and surfactant injected was accomplished to calculate the mass of each species extracted according to Eq (3)

$$m_{j\ extracted} = \int_0^{9.58\ h} Q_{ext} C_j dt \tag{3}$$

where m is the mass of j extracted at well PS14B from the beginning to the end of the extraction event (9.58 h), j is related to surfactant (g L^{-1}) or bromide (mg L^{-1}), Q_{ext} (L h^{-1}) is the corresponding flow rate of GW extracted at PS14B at time t, C_j is the concentration of j at time t, and t is the corresponding time (h) during the extraction event. Values of Q_{ext} (as m^3 h^{-1}) with time during the extraction event have been summarized in Table SI-1.

Fig. 5. Photograph of the DNAPL in emulsion extracted at the sampling point located at the bottom of the alluvium (16 m b g.l) in well PS14D 40 min after the injection had stopped.

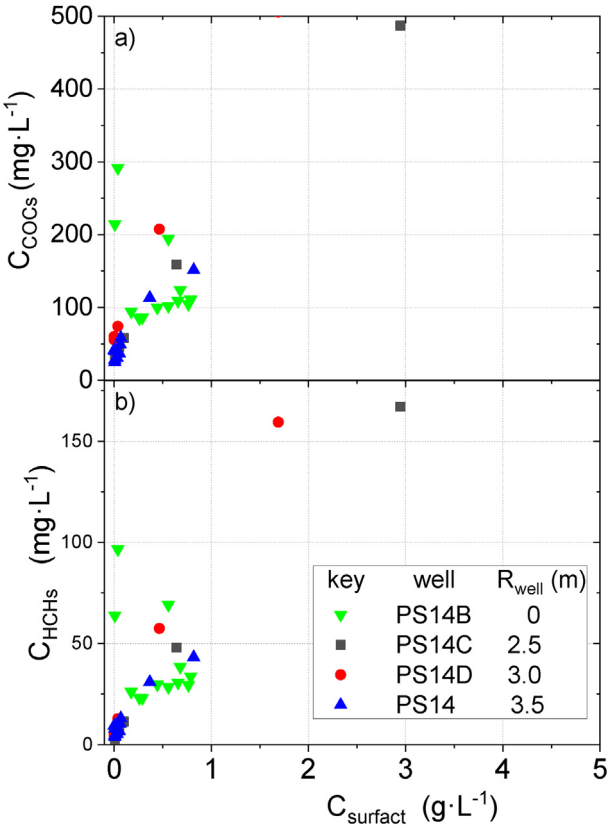

Fig. 6. COCs (a) and HCHs (b) concentration profiles with surfactant concentration in the GW samples during extraction in PS14B.

The volume of the aqueous phase injected or extracted was determined as the integral of the flow rate over time, according to Eq. (4)

$$V = \int_0^t Q_{PS14B} C_j dt \quad (4)$$

The mass of the conservative tracer (bromide) and the surfactant recovered in GW extraction is shown in Table 2. In spite of the fact that about double the volume of the aqueous phase was extracted in relation to the aqueous volume injected, only 52% of the tracer and about 9% of the surfactant injected was recovered. The low bromide recovered can be explained by the high dispersion of the fluid injected and extracted, as can be deduced from profiles in Fig. 4 and Table SI-2. In fact, a typical tail of high dispersion is noticed in the bromide concentration profile in Table SI-2, where the bromide concentration is still high (23.9 mg L^{-1}) at the end of the extraction. Furthermore, the recovery of the surfactant was quite low, much lower than bromide recovery, which is related to the selective surfactant adsorption in the soil or selective surfactant absorption in the DNAPL trapped in the soil pores. As shown in Fig. 6, COC concentration in the groundwater decreases at the same time as the surfactant in the aqueous phase.

3.4. Profiles of the species in the test cell of the alluvial layer during washing with tap water

As explained in the experimental section, two washes were carried out by injecting tap water in PS14, PS14C and PS14D and simultaneously extracting from PS14B a flow rate higher than the sum of the flow rates injected. The timetable is summarized in Table SI-1 and the profiles obtained are shown in Table 3. The results show that the surface tension measured in wells PS14, PS14C and PS14D after the first wash tended to achieve the ST value of the tap water. Since the surfactant solution was injected in PS14B, the lowest ST over time was obtained in this well. However, the surfactant concentration and the concentrations of COCs dissolved in PS14B were also quite low. Accordingly, the COCs and HCHs dissolved in the aqueous phase decrease over time. The values of concentration of COCs and HCHs dissolved during washing in the four wells were even lower than the values measured at the site before the injection of the surfactant.

Since the tracer was injected in well PS14B, the highest bromide concentration was obtained in this well. However, at the end of the second wash, the bromide in the GW samples in PS14B was close to 0.

A mass balance of the recovered bromide and surfactant in PS14B during washing was carried out by using Eq. (3). Looking at the values in Table 3, only the first wash with tap water was taken into account. The results are summarized in Table 4. In this table, the total bromide and surfactant percentages of the injected amounts recovered after GW extraction (Table 2) and the first wash with tap water are also provided. According to the figures, about 90% of the bromide injected was recovered but only 9% of the surfactant, confirming the selective and irreversible adsorption of the surfactant into the soil.

3.5. Groundwater monitoring

After the second wash with tap water, the concentration of COCs, HCHs and chloride as well as the conductivity in the GW samples of the four wells in the test cell were lower than the values measured before the surfactant was injected, as shown in Table 3. This is because water with low conductivity, chloride and COC concentrations was injected in the test cell during washing.

However, as mentioned before, only a small fraction of soil contamination in the alluvial layer of the test cell (<3%) was removed with the surfactant injection. While the natural groundwater flow in the alluvial layer is quite low (average Darcy velocity about 0.02 m day^{-1}), an equilibrium between the COCs adsorbed into the soil and dissolved in the aqueous phase will be reached over time. Additionally, contaminated groundwater enters the test cell after washing. Therefore, after washing, a rise in the COCs will be expected over time in wells PS14, PS14B, PS14C and PS14SD.

Table 2
Recovery of bromide and surfactant injected at the end of GW extraction.

$V_{injected}$ (m^3)	$Br^-_{injected}$ (g)	$Surfact_{injected}$ (kg)	$V_{extracted}$ (m^3)	$Br^-_{extracted}$ (g)	$Surfact._{extracted}$ (kg)	% Br^- injected recovered	% $Surfact._{injected\ recovered}$
5.28	686.4	68.64	9.65	386	6	56.2	8.86

Table 3
Analysis of GW samples in wells PS14B, PS14, PS14C and PS14D (depth of 14.5 m b g.l.) during washing with tap water. Values related as at the end of extraction correspond to those obtained at 9.58 h of GW extraction in Table SI-2.

t (h)	PS14A	k (mS cm^{-1})	ST (mN m^{-1})	Cl (mg L^{-1})	Br (mg L^{-1})	$C_{surfact}$ (g L^{-1})	COCs (mg L^{-1})	HCHs (mg L^{-1})
	End of Ext.	4629	41	896.54	3	0.006	49.62	10.36
0*	Wash1	5078	42	1083	2	0.07	83.38	18.38
1	Wash 1	4516	54	851	1.38	0	32.95	5.68
2	Wash1	312	68	126	0.5	0	6.94	1.42
3	Wash1	316.2	68.5	125	0	0	7.02	1.83
6	Wash1	329.6	63.5	127	0	0	18.73	4.02
0	Wash 2	2056	64	408	b.d.l.	0	6.4	2.7
6	Wash 2	434	70	138	b.d.l.	0	6.7	3.5
t (h)	PS14B	k (mS cm^{-1})	ST (mN m^{-1})	Cl (mg L^{-1})	Br (mg L^{-1})	$C_{surfact}$ (g L^{-1})	COCs (mg L^{-1})	HCHs (mg L^{-1})
	End of Ext.	4781	44	961	23.9	0.007	214.33	63.82
0*	Wash 1	4621	36.5	967	23.0	0.02	58.78	11.48
0.5	Wash1	4740	41	982	22.4	0.03	41.74	7.32
1	Wash1	4898	41	1051	20.7	0.02	36.75	4.61
1.5	Wash1	4442	43	739	16.1	0.01	31.69	3.74
2	Wash1	4012	43	840	13.1	0.01	31.52	3.65
2.5	Wash1	3650	44	767	10.6	0.01	32.45	3.09
3	Wash1	3428	45	709	8.8	0.01	31.35	3.08
3.5	Wash1	3354	45.5	689	7.8	0.01	33.51	2.88
4	Wash1	3160	47	645	6.6	0.01	31.24	2.87
4.5	Wash1	2974	47	606	5.5	0.01	30.34	1.99
5.5	Wash1	2810	47	566	4.4	0.01	26	3.14
0	Wash 2	2991	45	630	3.5	0	7.13	1.86
6	Wash 2	2657	50	529	2.0	0	6.5	1.15
t (h)	PS14C	k (mS cm^{-1})	ST (mN m^{-1})	Cl (mg L^{-1})	Br (mg L^{-1})	$C_{surfact}$ (g L^{-1})	COCs (mg L^{-1})	HCHs (mg L^{-1})
	End of Ext.	5314	41	1227	9.2	0.015	38.4	5.15
0*	Wash1	4821	41	1066	7	0.03	43.98	7.07
1	Wash 1	5580	46.5	1179	6	0	38	5.15
2	Wash1	296.4	59	124	0.5	0	8.47	2.45
3	Wash1	308.7	69	124	b.d.l.	0	6.66	2.26
6	Wash1	374.6	59	131	b.d.l.	0	8.66	1.18
0	Wash 2	2300	56	166	b.d.l.	0	5.0	0.8
6	Wash 2	412.2	70	236	b.d.l.	0	2.3	0.5
t (h)	PS14D	k (mS cm^{-1})	ST (mN m^{-1})	Cl (mg L^{-1})	Br (mg L^{-1})	$C_{surfact}$ (g L^{-1})	COCs (mg L^{-1})	HCHs (mg L^{-1})
	End of Ext.	5760	49	1335	7.26	0.007	58.51	4.71
0*	Wash1	5540	38	1303	6	0.41	160.5	39.2
1	Wash 1	6026	49	1437	5	0	72.1	7.7
2	Wash1	312	59	127	0.6	0	18.5	4
3	Wash1	482	60	147	0.2	0	24.1	4.5
6	Wash 1	885	53	204	b.d.l.	0	29.1	5.3
0	Wash 2	5345	51	1111	1	0	7.8	4.1
6	Wash 2	1247	59	236	0.8	0	9.2	4.6

* Time 0 in washing corresponds to the beginning of extraction in PS14B. The injection of tap water in PS14, PS14C and PS14D starts 1 h after the extraction in PS14B begins. b.d.l. means below the detection limit with the calibrate used.

Table 4
Recovery of bromide and surfactant after washing with tap water and total recovery considering previous extraction in Table 2.

$V_{extracted\ Wash\ 1\ 1}$ (m^3)	$V_{injected\ Wash\ 1\ 1}$ (m^3)	$Br^-_{Extracted\ wash\ 1}$ (g)	$Surfac_{extracted}$ (kg)	% Br^- injected recovered in washing 1	% Surfactant injected recovered in washing 1	Total % $Br^-_{injected}$ recovered	Total % $Surfactant_{injected\ recovered}$
20.9	12.76	227.62	0.25	25.7	0.3	89	9.16

As the surfactant was adsorbed into the test cell, its effect on the COCs dissolved over time should be evaluated. To do this, all of the wells were monitored for 30 days after washing and results were compared with concentration of HCHs monitored in the GW samples taken prior to the injection of the surfactant (April 18). As the results in Fig. 7 show, the injection of surfactant and further GW extraction and washing with tap water did not cause a rise in HCH concentration.

Other wells in the vicinity of the test cell and in the direction of the natural GW flow were monitored up to 4 months after the injection of surfactant and compared with the values prior to this. The results are

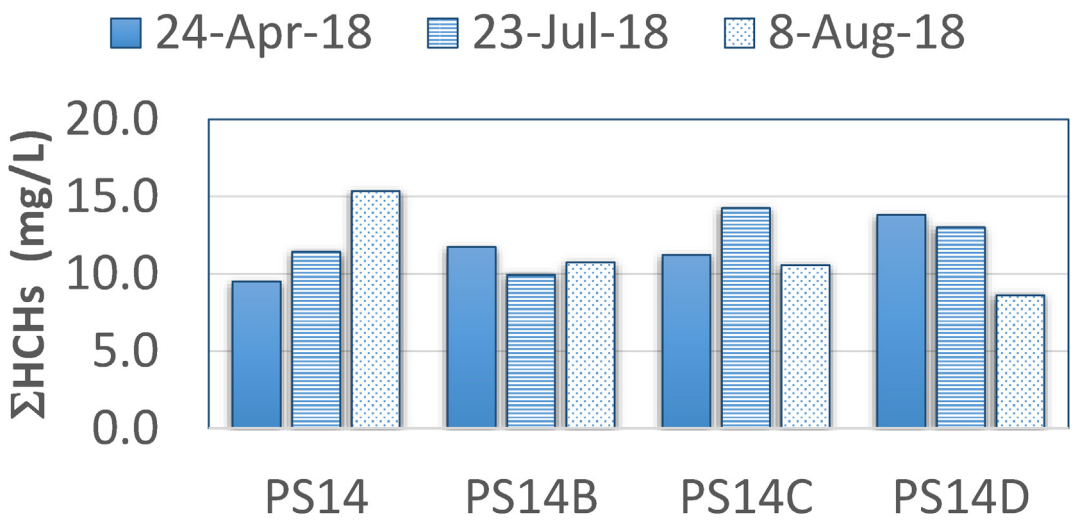

Fig. 7. Profiles of HCHs in April–July - August 2018. Injection of surfactant carried out on 10-7-2018.

shown in Fig. 8 and show that, no rise in the HCH concentration was noticed after the injection and extraction of surfactant and washing.

4. Conclusions

An aqueous solution of a non-ionic and biodegradable surfactant and a tracer (bromide) was injected at the Sardas Landfill (Sabiñanigo, Spain) with the subsequent extraction of groundwater and washing with tap water to recover the chemicals injected. Based on the results, the following conclusions have been reached:

The radial dispersion of the injected fluids was high The contribution of radial dispersion to the transport of the injected fluid was remarkable, as can be deduced from the profiles shown in Fig. 2. The concentration of surfactant and bromide in the three monitoring wells began to rise at short times after the injection of these compounds in well PS14B, these times being much lower than those calculated in advective flow (t_{FP}). Therefore, the contribution of the radial dispersive component of the flow was significant and the advective flow model cannot be used to predict the profiles of the chemical injected with regard to time and position. Moreover, high radial dispersion of the flow was also noticed during groundwater extraction. The high dispersion component of the flow in the alluvium is explained by the high permeability of the gravel and sand layer. Also, a much larger volume of the fluid injected must be extracted to recover the chemicals. This should be taken into account when a full-scale remediation process is designed, since the chemicals injected may be quickly diluted with the GW found on site.

The surfactant was not adsorbed during injection but in the period of time (15 h) between injection and extraction. Contact time and flow speed are key parameters in the design of the SEAR process. Surfactant adsorption when the injection flow stops is probably related to the clay content interbedded in the gravel-sand layer. It was found that the partition equilibrium between COCs in soil and GW was achieved in about 60 min. The solubilization of COCs in equilibrium conditions allowed for the elimination of about 3.5 % of COCs in the soil using the pore volume of the surfactant aqueous solution (effective porosity of soil is less than 0.12). The moderate concentration of COCs dissolved at equilibrium in the groundwater (about 850 mg L^{-1}) is related to the moderate average contamination of the soil in the test cell (about 1230 mg kg^{-1}). The optimal treatment for soil flushing seems to be successive injections of small volumes of the surfactant solution and extraction after a short contact time (1–2 h), although other alternatives such as S–ISCO should be evaluated.

In contrast, the extraction of the free DNAPL in the altered marls was greatly facilitated with the addition of surfactant, and the DNAPL was easily emulsified. Therefore, the depths chosen for the injection of the surfactant aqueous solution and the subsequent GW extraction should be close to the area with high DNAPL concentration (in this case in the contact area between the gravel and the altered marl layers).

Finally, it was found that the surfactant and the contamination did not migrate from the capture zone. The irreversible adsorption of surfactant in the absence of an injection flow helps to control the dispersion of contamination because the concentration of COCs in the solution decreases as the surfactant concentration decreases. Moreover, surface tension cannot be used as the only parameter to follow the progress of the fluid injected when the CMC of the surfactant employed is quite low.

Declarations

Author contribution statement

Aurora Santos & David. Lorenzo: Conceived and designed the experiments; Analyzed and interpreted the data; Contributed reagents, materials, analysis tools or data; Wrote the paper.

Carmen.M Domínguez & Miguel A. Lominchar: Performed the experiments; Analyzed and interpreted the data; Contributed reagents, materials, analysis tools or data; Wrote the paper.

Raul. García-Cervilla & Jorge Gómez: Performed the experiments; Analyzed and interpreted the data; Contributed reagents, materials, analysis tools or data.

Jesús Fernández & Joaquín Guadaño: Conceived and designed the experiments; Analyzed and interpreted the data; Contributed reagents, materials, analysis tools or data.

Funding statement

This work was supported by the Regional Government of Madrid, project CARESOIL (S2018/EMT-4317) and by the Spanish Ministry of Economy, Industry and Competitiveness, project CTM2016-77151-C2-1-R. The authors thank the Department of Agriculture, Livestock and Environment, Government of Aragon, Spain, as well as EMGRISA for their support during this work.

Competing interest statement

The authors declare no conflict of interest.

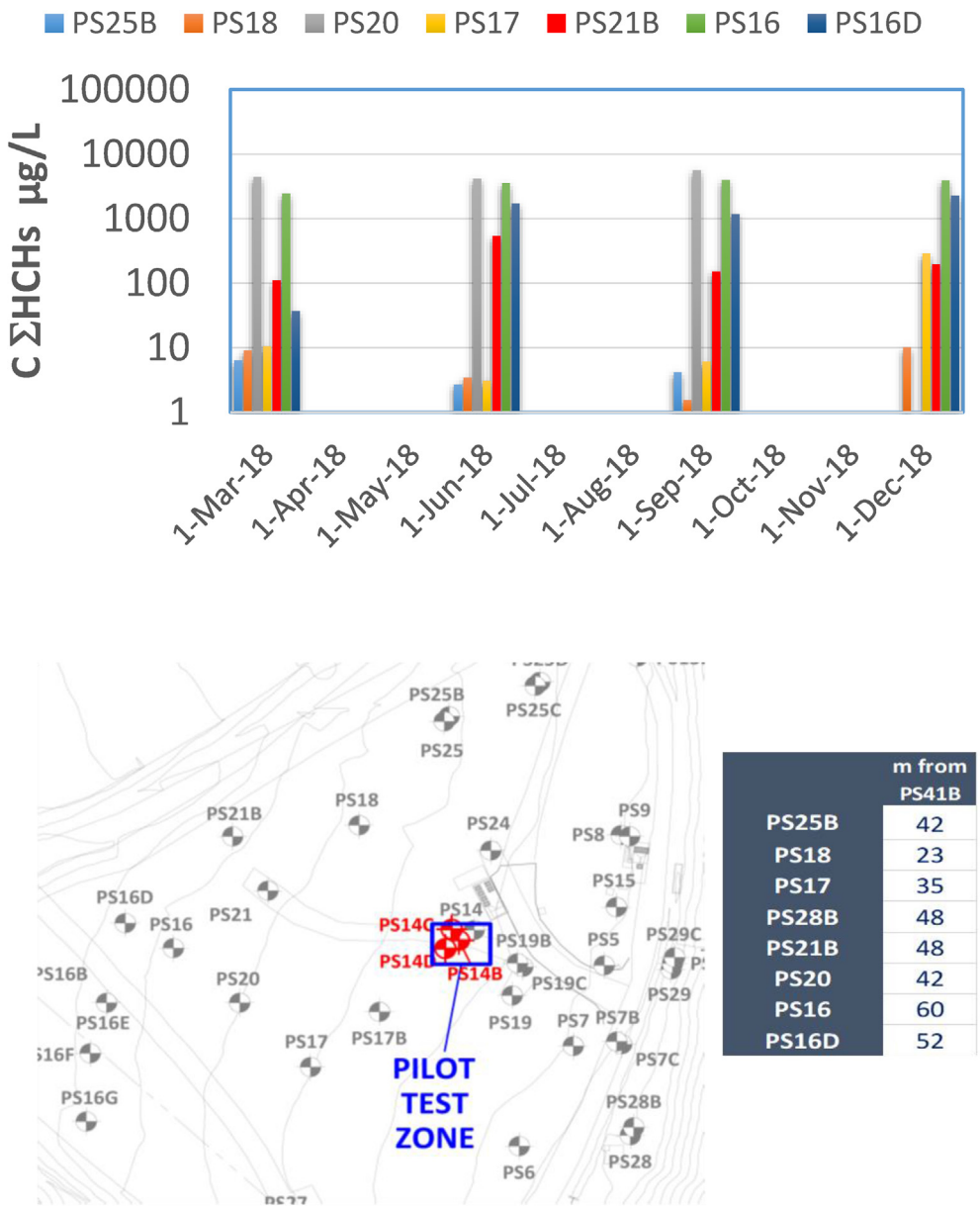

Fig. 8. Monitoring of GW in wells located in the alluvium in the vicinity of the test cell over time in the direction of the groundwater flow.

Additional information

Supplementary content related to this article has been published online at https://doi.org/10.1016/j.heliyon.2019.e02875.

References

Abriola, L.M., Drummond, C.D., Hahn, E.J., Hayes, K.F., Kibbey, T.C.G., Lemke, L.D., et al., 2005a. Pilot-scale demonstration of surfactant-enhanced PCE solubilization at the Bachman road site. 1. Site characterization and test design. Environ. Sci. Technol. 39, 1778–1790.

Acosta, E.J., Quraishi, S., 2014. Surfactant technologies for remediation of oil spills. In: Somasundaran, P., Patra, P., Farinato, R.S., Papadopoulos, K. (Eds.), Oil Spill Remediation: Colloid Chemistry-Based Principles and Solutions. Wiley, pp. 317–358.

Agaoglu, B., Copty, N.K., Scheytt, T., Hinkelmann, R., 2015. Interphase mass transfer between fluids in subsurface formations: a review. Adv. Water Resour. 79, 162–194.

Atteia, O., Estrada, E.D., Bertin, H., Dec 2013. Soil flushing: a review of the origin of efficiency variability. In: Reviews in Environmental Science and Bio/Technology, 12. Springer, pp. 379–389.

Aydin, G.A., Agaoglu, B., Kocasoy, G., Copty, N.K., 2011. Effect of temperature on cosolvent flooding for the enhanced solubilization and mobilization of NAPLs in porous media. J. Hazard Mater. 186, 636–644.

Besha, A.T., Bekele, D.N., Naidu, R., Chadalavada, S., 2018. Recent advances in surfactant-enhanced In-Situ Chemical Oxidation for the remediation of non-aqueous phase liquid contaminated soils and aquifers. Environ. Technol. Innovat 9, 303–322.

Brebbia, C.A., 2013. Sustainable Development and Planning VI. 173. Wit Press, Southampton, UK, pp. 661–671.

Brusseau, M.L., 2013. The Impact of DNAPL Source-Zone Architecture on Contaminant Mass Flux and Plume Evolution in Heterogeneous Porous media. ARIZONA UNIV TUCSON.

Cheng, M., Zeng, G.M., Huang, D.L., Yang, C.P., Lai, C., Zhang, C., et al., 2017. Advantages and challenges of Tween 80 surfactant-enhanced technologies for the remediation of soils contaminated with hydrophobic organic compounds. Chem. Eng. J. 314, 98–113.

CLU-IN, 2016. Dense Nonaqueous Phase Liquids (Dnapls), 2016. Clu-in.

Collins, J., 2012. Coal tar contamination remediation. Pollulation Eng. 44, 26–30.

Council, N.R., 2013. Alternatives for Managing the Nation's Complex Contaminated Groundwater Sites. National Academies Press.

Dominguez, C.M., Romero, A., Santos, A., 2019. Selective removal of chlorinated organic compounds from lindane wastes by combination of nonionic surfactant soil flushing and Fenton oxidation. Chem. Eng. J. 376, 120009.

Dugan, P.J., Siegrist, R.L., Crimi, M.L., 2010. Coupling surfactants/cosolvents with oxidants for enhanced DNAPL removal: a review. Remediat. J. 20, 27–49.

EthicalChem, 2016d. SEPR and S-ISCO Remediation of Creosote Bridgeville. Delaware, York. 2019.

EthicalChem, 2016e. SEPR and S-ISCO Remediation of MGP Gasworks. Sydney Australia. 2019.

EthicalChem, 2019. Remediation Case Studies. Available in. https://www.ethicalchem.com/remediation-case-studies (Visited in October 2019).
Fernández, J., Arjol, M., Cacho, C., 2013. POP-contaminated sites from HCH production in Sabiñánigo, Spain. Environ. Sci. Pollut. Control Ser. 20, 1937–1950.
Henry, S.M., Hardcastle, C.H., Warner, S.D. J.C.s., remediation, D., 2003. Chlorinated solvent and DNAPL remediation: an overview of physical. chemical, and biological processes 837, 1–20.
Hoag, G.E., Collins, J., 2011. Soil remediation method and composition. Google Patents.
Kang, S., Lim, H.S., Gao, Y., Kang, J., Jeong, H.Y., 2019. Evaluation of ethoxylated nonionic surfactants for solubilization of chlorinated organic phases: effects of partitioning loss and macroemulsion formation. J. Contam. Hydrol. 223.
Koch, J., Nowak, W., 2015. Predicting DNAPL mass discharge and contaminated site longevity probabilities: conceptual model and high-resolution stochastic simulation. Feb 51, 806–831.
Kokkinaki, A., O'Carroll, D.M., Werth, C.J., Sleep, B.E., 2013. Coupled simulation of DNAPL infiltration and dissolution in three-dimensional heterogeneous domains: process model validation. Feb 49, 7023–7036.
Lee, M., Kang, H., Do, W., 2005. Application of nonionic surfactant-enhanced in situ flushing to a diesel contaminated site. Water Res. 39, 139–146.
Lominchar, M.A., Lorenzo, D., Romero, A., Santos, A., 2018. Remediation of soil contaminated by PAHs and TPH using alkaline activated persulfate enhanced by surfactant addition at flow conditions. J. Chem. Technol. Biotechnol. 93, 1270–1278.
Londergan, J., Yeh, L., 2003. Surfactant-Enhanced Aquifer Remediation (SEAR) Implementation Manual. INTERA INC AUSTIN TX.
Luciano, A., Mancini, G., Torretta, V., Viotti, P., 2018. An empirical model for the evaluation of the dissolution rate from a DNAPL-contaminated area. Environ. Sci. Pollut. Res. 25, 33992–34004.
Maire, J., Coyer, A., Fatin-Rouge, N., 2015. Surfactant foam technology for in situ removal of heavy chlorinated compounds-DNAPLs. J. Hazard Mater. 299, 630–638.
Maire, J., Joubert, A., Kaifas, D., Invernizzi, T., Marduel, J., Colombano, S., et al., 2018. Assessment of flushing methods for the removal of heavy chlorinated compounds DNAPL in an alluvial aquifer. Sci. Total Environ. 612, 1149–1158.
Mao, X., Jiang, R., Xiao, W., Yu, J., 2015a. Use of surfactants for the remediation of contaminated soils: a review. J. Hazard Mater. 285, 419–435.
Mao, X.H., Jiang, R., Xiao, W., Yu, J.G., 2015b. Use of surfactants for the remediation of contaminated soils: a review. J. Hazard Mater. 285, 419–435.
McGuire, T.M., McDade, J.M., Newell, C.J.J.G.M., 2006. Remediation. In: Performance of DNAPL source depletion technologies at 59 chlorinated solvent-impacted sites, 26, pp. 73–84.
Muherei, M.A., Junin, R., Bin Merdhah, A.B., 2009. Adsorption of sodium dodecyl sulfate, Triton X100 and their mixtures to shale and sandstone: a comparative study. J. Pet. Sci. Eng. 67, 149–154.
Mulligan, C., Yong, R., Gibbs, B., 2001. Surfactant-enhanced remediation of contaminated soil: a review. Eng. Geol. 60, 371–380.
Nas, M.S., Kuyuldar, E., Demirkan, B., Calimli, M.H., Demirbaş, O., Sen, F., 2019. Magnetic nanocomposites decorated on multiwalled carbon nanotube for removal of Maxilon Blue 5G using the sono-Fenton method. Sci. Rep. 9, 10850.
Paria, S., 2008. Surfactant-enhanced remediation of organic contaminated soil and water. Apr 138, 24–58.
Sahoo, D., Smith, J.A., Imbrigiotta, T.E., McLellan, H.M., 1998. Surfactant-enhanced remediation of a trichloroethene-contaminated aquifer. 2. Transport of TCE. Environmental Science & Technology 32, 1686–1693.
Santos, A., Fernandez, J., Guadano, J., Lorenzo, D., Romero, A., 2018a. Chlorinated organic compounds in liquid wastes (DNAPL) from lindane production dumped in landfills in Sabinanigo (Spain). Environ. Pollut. 242, 1616–1624.
Şen, F., Demirbaş, Ö., Çalımlı, M.H., Aygün, A., Alma, M.H., Nas, M.S., 2018. The dye removal from aqueous solution using polymer composite films. Appl. Water Sci. 8, 206.
Siegrist, R.L., Crimi, M., Simpkin, T.J., 2011a. Situ Chemical Oxidation for Groundwater Remediation. Springer-Verlag, New York. New York.
Siegrist, R.L., Crimi, M., Simpkin, T.J., 2011b. In Situ Chemical Oxidation for Groundwater Remediation, 3. Springer Science & Business Media.
Strbak, L., 2000. Situ flushing with Surfactants and Cosolvents. National Network of Environmental Studies Fellowship Report for US Environmental Protection Agency, Office of Solid Waste and Emergency Response Technology Innovation Office, Washington, DC.
Stroo, H.F., Leeson, A., Marqusee, J.A., Johnson, P.C., Ward, C.H., Kavanaugh, M.C., et al., 2012. Chlorinated ethene source remediation: lessons learned. Environ. Sci. Technol. 46, 6438–6447.
Svab, M., Kubala, M., Muellerova, M., Raschman, R., 2009. Soil flushing by surfactant solution: pilot-scale demonstration of complete technology. J. Hazard Mater. 163, 410–417.
van Liedekerke, M., Prokop, G., Rabl-Berger, S., Kibblewhite, M., Louwagie, G., 2014. Progress in the Management of Contaminated Sites in Europe.
Wang, W.H., Hoag, G.E., Collins, J.B., Naidu, R., 2013. Evaluation of surfactant-enhanced in situ chemical oxidation (S-ISCO) in contaminated soil. Water Air Soil Pollut. 224, 1–9.